A CD146 FACS PROTOCOL ENRICHES FOR LUMINAL KERATIN 14/19 DOUBLE POSITIVE HUMAN BREAST PROGENITORS

Ólöf Gerdur Ísberg, Jiyoung Kim, Agla J. Fridriksdottir, Mikkel Morsing, Vera Timmermans-Wielenga, Lone Rønnov-Jessen, Ole William Petersen & René Villadsen

Supplementary Information:

Supplementary Figures

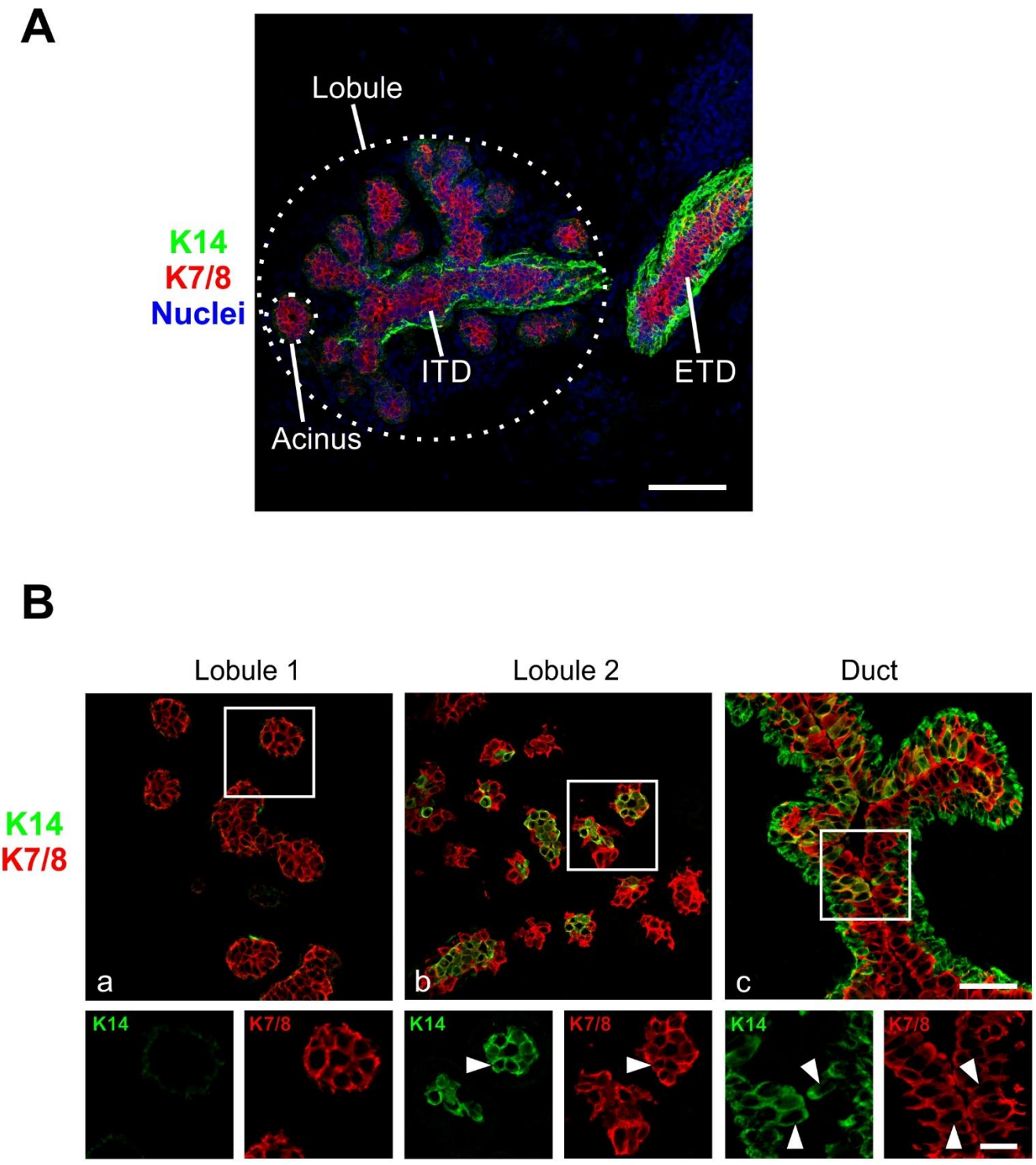

Supplementary Figure S1. Keratin 14^+ DP cells can be found in distinct profiles of the human breast gland. (A) Immunofluorescent staining of human breast gland by K14 (green) and K7/8 (red). Nuclei are stained in blue. The adult human breast gland can be divided into lobular and ductal structures. A lobule consists of an intralobular duct (ITD) that braches into a number of ductules/acini. The ITD is connected to the extralobular duct (ETD) outside the lobular structure. Note that the basal cells of the ducts generally strongly express K14, while the myoepithelium in the acini often shows diminished staining. Bar, 100 µm. (B) Immunofluorescent staining performed as above demonstrating examples of the distribution of DP cells in lobules (a, b) and ducts (c). Image subsets are marked and shown in single color channels, and arrowheads mark examples of DP cells. While $K14^+$ DP cells are most prominently found in ducts, occasionally DP cells are observed in lobular acini. Bar, 50 µm. Image subsets, bar, 20 µm.

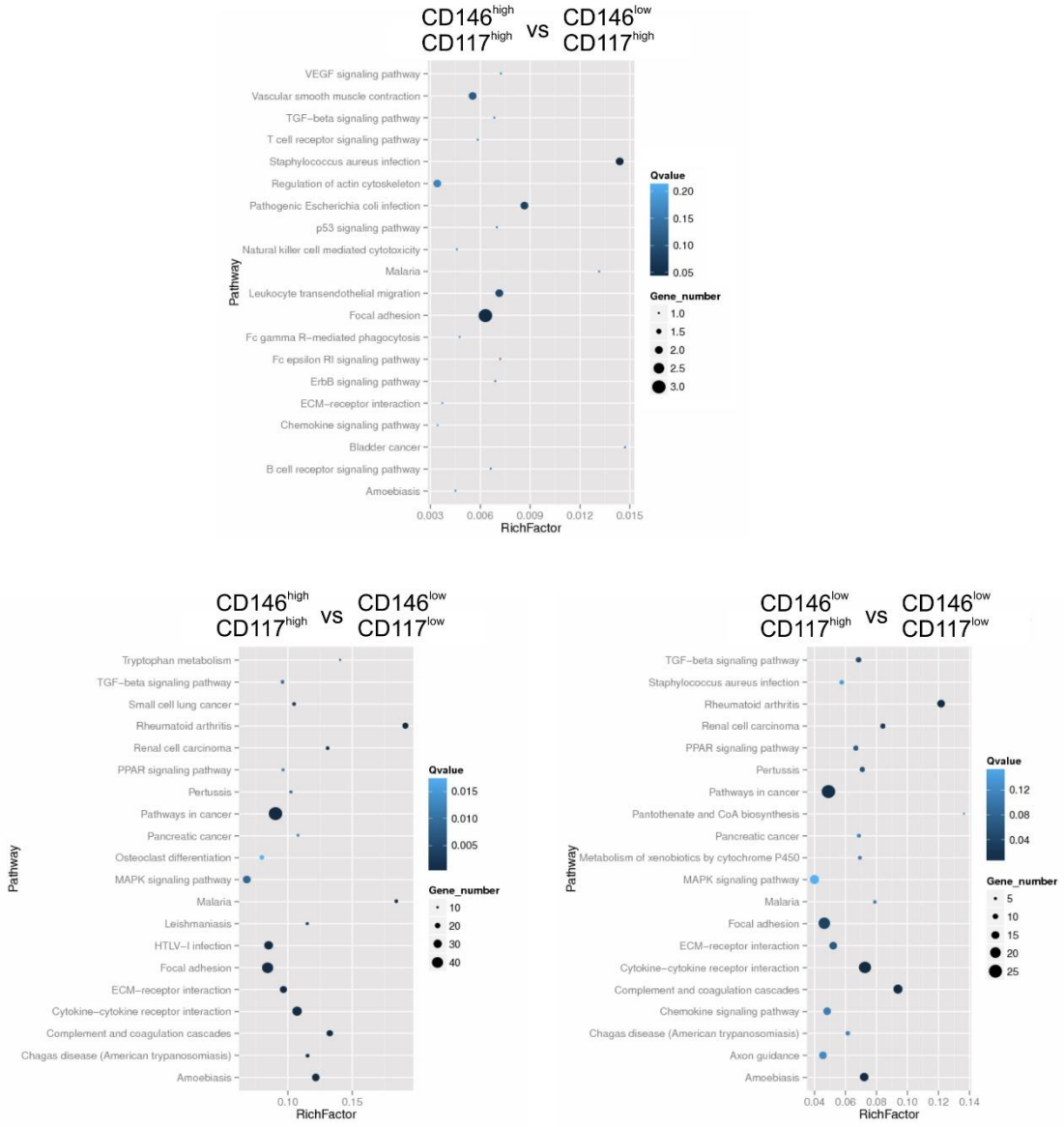

Supplementary Figure S2. Classification of gene expression patterns from RNA-Seq data reveals subtle differences between the sorted epithelial subpopulations. Scatter plots of KEGG pathway enrichment statistics, comparing CD146^{high}/CD117^{high} with CD146^{low}/CD117^{high} and CD146^{low}/CD117^{low} as well as CD146^{low}/CD117^{high} with CD146^{low}/CD117^{low}. Rich Factor indicates the ratio between DEGs and the number of genes annotated in the given pathway. Q Value indicates adjusted p value depicting significant enrichment (Q value < 0.05, navy blue).

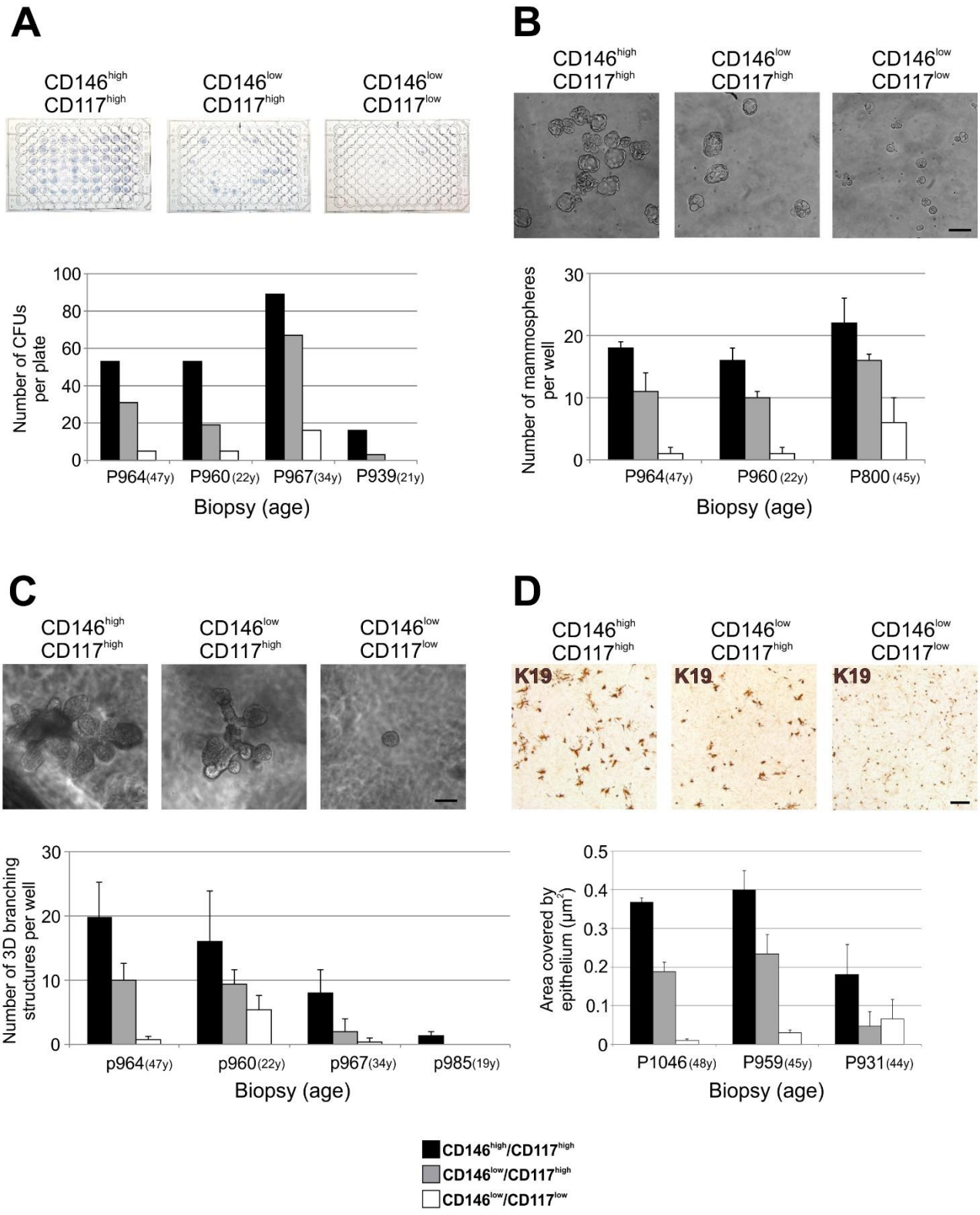
A
CD146high CD117high
CD146low CD117high
CD146low CD117low
Number of CFUs per plate
100
80
60
40
20
0
P964(47y)
P960(22y)
P967(34y)
P939(21y)
Biopsy (age)
B
CD146high CD117high
CD146low CD117high
CD146low CD117low
Number of mammospheres per well
30
20
10
0
P964(47y)
P960(22y)
P800(45y)
Biopsy (age)
C
CD146high CD117high
CD146low CD117high
CD146low CD117low
Number of 3D branching structures per well
30
20
10
0
p964(47y)
p960(22y)
p967(34y)
p985(19y)
Biopsy (age)
D
CD146high CD117high
CD146low CD117high
CD146low CD117low
K19
K19
K19
Area covered by epithelium (µm2)
0.5
0.4
0.3
0.2
0.1
0
P1046(48y)
P959(45y)
P931(44y)
Biopsy (age)
CD146high/CD117high
CD146low/CD117high
CD146low/CD117low

Supplementary Figure S3. CD146^{high}/CD117^{high}, CD146^{low}/CD117^{high} and CD146^{low}/CD117^{low} cells differ in functional assays of progenitor activity. For each assay, representative images of cells/structures are shown along with bar diagrams of quantitative data (CD146^{high}/CD117^{high} (black bars), CD146^{low}/CD117^{high} (grey bars), CD146^{low}/CD117^{low} (white bars)) from the biopsies tested. The graphs detail the data presented collectively in Figure 3B. (A) Colony forming unit (CFU) assay with directly sorting 10 cells per well with into one 96 well plate per population. (B) Mammosphere assay with 5,000 cells per well in triplicate for each population. Bar, 100 μm. (C) 3D morphogenesis assay with 20,000 cells per well in triplicate for each population inoculated in Matrigel. Bar, 100 μm. (D) Branching morphogenesis upon epithelial-stromal interaction with 5,000 cells per flask seeded onto CD105^{high} fibroblast feeders in triplicate. Bar, 250 μm. Irrespective of the biopsy tested, the CD146^{high}/CD117^{high}cells exhibit the highest progenitor cell activity. Error bars indicate SDs.

Supplementary tables

Supplementary Table S1. Quantification of the presence of $K14^+$ luminal cells in 40 normal breast gland structures, divided into lobules and ducts. Structures were evaluated based on immunoperoxidase stainings of tissue sections. A structure was determined $K14^+$ when one or more luminal cells within the structure were identified as positive. Data are included in Figure 1 and Figure 4B.

No.	Biopsy ID	Age (years)	Structural location	Total structures	$K14^+$	% positive
1	P648	13	lobules	11	0	0
2	W430/3	15	lobules	3	0	0
3	W428/1	17	lobules	27	0	0
4	W430/1	17	lobules	10	0	0
5	W466/3	18	lobules	9	0	0
6	P790	18	lobules	9	0	0
7	P944	18	lobules	13	1	7.7
8	P1094	18	lobules	13	0	0
9	F526	19	lobules	6	0	0
10	W403/2	19	lobules	14	0	0
11	P816	20	lobules	35	1	2.9
12	P652	20	lobules	5	0	0
13	W562/1	21	lobules	6	0	0
14	W458/1	22	lobules	5	0	0
15	W1908/3	23	lobules	11	0	0
16	F518	24	lobules	10	1	10
17	P644	25	lobules	11	0	0
18	W1916/6	27	lobules	10	1	10
19	P645	29	lobules	10	2	20
20	P820	29	lobules	12	1	8.3
21	P672	30	lobules	8	1	12.5
22	P832	32	lobules	12	8	66.7
23	P683	33	lobules	15	2	13.3
24	P636	34	lobules	20	1	5.0
25	P671	36	lobules	43	13	30.2
26	P809	39	lobules	9	7	77.8
27	P653	41	lobules	8	0	0
28	P880	43	lobules	7	1	14.3
29	W901	43	lobules	15	3	20
30	P659	43	lobules	9	0	0
31	P819	45	lobules	12	2	16.7
32	F498	46	lobules	20	2	10
33	W438	49	lobules	35	12	34.3
34	P637	49	lobules	24	5	20.8
35	W371/3	52	lobules	19	1	5.3
36	P634	56	lobules	10	5	50
37	P647	56	lobules	7	3	42.9
38	P940	59	lobules	6	0	0

39	W430/2	59	lobules	16	0	0
40	P828	74	lobules	7	0	0
1	P648	13	ducts	6	3	50
2	W430/3	15	ducts	3	3	100
3	W428/1	17	ducts	8	2	25
4	W430/1	17	ducts	11	6	54.5
5	W466/3	18	ducts	9	5	55.6
6	P790	18	ducts	6	3	50
7	P944	18	ducts	6	3	50
8	P1094	18	ducts	10	3	30
9	F526	19	ducts	5	3	60
10	W403/2	19	ducts	9	2	22.2
11	P816	20	ducts	8	3	37.5
12	P652	20	ducts	6	1	16.7
13	W562/1	21	ducts	6	1	16.7
14	W458/1	22	ducts	14	6	42.9
15	W1908/3	23	ducts	8	4	50
16	F518	24	ducts	6	1	16.7
17	P644	25	ducts	12	4	33.3
18	W1916/6	27	ducts	6	5	83.3
19	P645	29	ducts	4	2	50
20	P820	29	ducts	11	6	54.5
21	P672	30	ducts	7	2	28.6
22	P832	32	ducts	7	5	71.4
23	P683	33	ducts	9	6	66.7
24	P636	34	ducts	17	10	58.8
25	P671	36	ducts	21	12	57.1
26	P809	39	ducts	7	7	100
27	P653	41	ducts	5	1	20
28	P880	43	ducts	6	4	66.7
29	W901	43	ducts	9	5	55.6
30	P659	43	ducts	8	6	75.0
31	P819	45	ducts	8	6	75.0
32	F498	46	ducts	8	4	50
33	W438	49	ducts	14	11	78.6
34	P637	49	ducts	10	7	70.0
35	W371/3	52	ducts	14	13	92.9
36	P634	56	ducts	9	6	66.7
37	P647	56	ducts	6	6	100
38	P940	59	ducts	7	5	71.4
39	W430/2	59	ducts	9	1	11.1
40	P828	74	ducts	8	4	50

Supplementary Table S2. Quantification of $K14^+$ DP luminal cells in normal breast gland structures stained by double-labeling immunofluorescence with general luminal keratin marker CAM5.2 against K7/8. The number of unique structures evaluated for each biopsy is shown in parenthesis. In all 5 biopsies a higher proportion of DP cells was present in ducts.

No.	Biopsy ID	Age (years)	Structures	$K14^+$/total $K7/8^+$
1	P644	25	Lobules (5)	0/518 (0.0%)
			Ducts (7)	26/469 (5.5%)
2	P832	32	Lobules (5)	10/770 (1.3%)
			Ducts (5)	17/377 (4.5%)
3	P683	33	Lobules (7)	1/604 (0.2%)
			Ducts (3)	66/407 (16.2%)
4	P809	39	Lobules (4)	117/706 (16.6%)
			Ducts (5)	187/609 (30.7%)
5	W438	46	Lobules (4)	35/606 (5.8%)
			Ducts (4)	82/422 (19.4%)

Supplementary Table S3. Topological evaluation of CD146 expression in luminal cells in the normal breast gland by immunohistochemical staining of 20 biopsies. -, +, ++ and +++ are indications of the relative frequency of $CD146^+$ luminal cells. In 19 out of 20 biopsies, a more prominent CD146 expression was observed in ducts. * $p < 0.00001$, tested by Mann-Whitney test.

No.	Biopsy ID	Age (years)	Reaction in ducts*	Reaction in lobules	Most prominent in ducts
1	P648	13	++	+	•
2	W430/1	17	++	+	•
3	W445	20	++	+	•
4	P652	20	+++	-	•
5	P722	20	-	-	
6	W1908/3	23	+	-	•
7	P663	24	++	+	•
8	P644	25	+++	-	•
9	P820	29	++	+	•
10	P672	30	++	+	•
11	P683	33	+	-	•
12	P772	33	++	-	•
13	P636	34	+++	+	•
14	P671	36	+++	+	•
15	P653	40	+++	++	•
16	P633	45	+++	+	•
17	F498	46	++	+	•
18	W652	46	+	-	•
19	P637	49	++	+	•
20	P647	56	+	-	•

Supplementary Table S4. Relative distribution of $CD117^+$ and $CD146^+$ luminal cells in ducts and lobules from normal breast tissue in serial immunostained sections. +, ++ and +++ are indications of the relative frequency of $CD117^+$ cells compared to $CD146^+$ cells. In all eight biopsies a higher frequency of $CD117^+$ cells was observed in ducts and lobules. * $p < 0.01$, tested by Mann-Whitney test.

No.	Biopsy ID	Age (years)	Ducts, CD117/CD146 ratio*	Lobules, CD117/CD146 ratio
1	P652	20	+	+++
2	P820	29	++	+++
3	P683	33	++	+++
4	P772	33	++	+++
5	P671	36	++	++
6	P653	40	+	++
7	P633	45	++	+++
8	F498	46	+++	+++

Supplementary Tables S5-S8 are available as individual excel documents:

Supplementary Table S5. Summary of RNA sequencing data from CD146^{high}/CD117^{high} (CD146), CD146^{low}/CD117^{high} (CD117) and CD146^{low}/CD117^{low} (CD326) luminal populations from 3 biopsies (P960, P964 and P967) (mapping to reference genome).

Supplementary Table S6. RNA-seq data analysis of CD146^{high}/CD117^{high} (CD146), CD146^{low}/CD117^{high} (CD117) and CD146^{low}/CD117^{low} (CD326) luminal populations from 3 biopsies (P960, P964 and P967).

Supplementary Table S7. List of differently expressed genes by NOISeq comparing CD146^{high}/CD117^{high} vs CD146^{low}/CD117^{high}, CD146^{low}/CD117^{low} vs CD146^{high}/CD117^{high} and CD146^{low}/CD117^{low} vs CD146^{low}/CD117^{high} populations.

Supplementary Table S8. Supplementary Table S8. Summary of gene ontology analysis of DEGs. A-C: Comparison of CD146^{high}/CD117^{high} (CD146) and CD146^{low}/CD117^{high} (CD117). D-F: Comparison of CD117 and CD146^{low}/CD117^{low} (CD326). G-I: Comparison of CD146 and CD326.

Supplementary Table S9. Quantification of the frequency of DP cells in smears of trypsinized primary breast tissue. Twenty biopsies were stained for K14/K19, and seven of these were additionally stained for K14/K7/8. The data are included in Figure 5A.

No.	Biopsy ID	Age	$K14^+$/total $K19^+$	$K14^+$/total $K7/8^+$
1	P985	19 years	7/831 (0.8%)	
2	P790	19 years	11/620 (1.8%)	7/633 (1.1%)
3	P722	20 years	27/600 (4.5%)	
4	P939	21 years	6/508 (1.2%)	
5	P960	22 years	58/1040 (5.6%)	59/1050 (5.6%)
6	P987	23 years	33/1020 (3.2%)	
7	P848	23 years	23/515 (4.5%)	19/532 (3.6%)
8	P749	25 years	24/571 (4.2%)	13/572 (2.3%)
9	P636	34 years	44/1000 (4.4%)	
10	P967	34 years	298/919 (32.4%)	
11	P640	35 years	21/596 (3.4%)	
12	P952	37 years	22/500 (4.4%)	
13	P966	41 years	68/1062 (6.4%)	70/1029 (6.8%)
14	P653	41 years	40/360 (11.1%)	
15	P727	44 years	25/570 (4.4%)	16/560 (2.9%)
16	P737	44 years	78/939 (8.3%)	49/974 (5.0%)
17	P964	47 years	92/579 (15.9%)	
18	P936	54 years	20/483 (4.1%)	
19	P937	54 years	81/562 (14.4%)	
20	P962	59 years	38/437 (8.7%)	

Supplementary Table S10. An overview of the presence of vDP cells in lobules and ducts of women with no known *BRCA1* mutations (normal) and of *BRCA1* mutation carriers. The predominant phenotype is marked with '●' in lobules and ducts for each biopsy. In cases where both phenotypes were found in equal amounts, both are marked. Cases where no vDP/DP cells were identified are marked with '-'. In general, lobules contain vDP cells while ducts have DP cells co-expressing CD146. For *BRCA1* mutation carriers age was not available (na).

			Lobules		Ducts	
		Age	vDP cells without CD146	DP cells with CD146	vDP cells without CD146	DP cells with CD146
Normal						
	W430/1	17	-	-		●
	W466/3	18	-	-		●
	P790/1	18	-	-		●
	P944	18	-	-		●
	W458/1	22	-	-		●
	F518	24	●			●
	P644	25	-	-		●
	W1916/6	27	-	-		●
	P832	32	●			●
	P636	34	-	-		●
	P671	36	●		●	
	P809	39	●			●
	W901	43	●			●
	W438	46		●		●
	P637	49	●		●	
	P634	56	●		●	●
BRCA1 mutation carriers						
	P705	na	-	-		●
	P714	na	●			●
	P728	na	●	●		●
	P734	na	●			●
	P742	na	●			●
	P744	na	●		●	
	P754	na	●			●
	P825	na	●			●
	P847	na	●			●
	P911	na	-	-		●

Supplementary Table S11. Quantification of the frequency of DP cells expressing Ki67 evaluated by immunofluorescence on tissue sections from normal women (normal) and *BRCA1* mutation carriers (BRCA1). It should be noted that the biopsies listed as normal are from women presumed not to have a BRCA1 mutation, as they were not tested. The average age of donor of normal breast biopsies was 44.6 years. For *BRCA1* mutation carriers information on age was not available (na). The data are included in Figure 6.

Status	Biopsy ID	Age (years)	$Ki67^+$-DP/total DP cells	%
normal	P647	56	0/174	0%
normal	W438	46	2/511	0.4%
normal	P832	32	0/273	0%
normal	P634	56	0/355	0%
normal	P671	36	10/439	2.3%
normal	P880	43	1/322	0.3%
normal	W901	43	0/283	0%
BRCA1 mutated	P714	na	11/167	6.6%
BRCA1 mutated	P734	na	4/221	1.8%
BRCA1 mutated	P744	na	6/544	1.1%
BRCA1 mutated	P754	na	8/443	1.8%
BRCA1 mutated	P825	na	4/252	1.6%
BRCA1 mutated	P847	na	1/398	0.3%
BRCA1 mutated	P852	na	3/124	2.4%

Supplementary Table S12. Overview of the CD146 status of tumors that are predominantly DP positive. Six carcinomas with >50% of DP neoplastic cells were selected from 23 ERα-negative tumors expressing K14. Five of the six tumors did not express CD146.

Tumor			vDP cells without CD146	DP cells with CD146
1	P860	-	●	
2	P914	-	●	
3	P942	-	●	
4	P994	-	●	
5	P1049	-	●	
6	W1884/3	-		●

Supplementary Table S13. List of antibodies used for immunostaining/FACS.

Antibody	**Clone**	**Company/Cat. no.**	**Peroxidase**	**Fluorescence**	**FACS**
α-smooth muscle actin	1A4	Sigma, A5691	-	1:500	-
CD117	K45	NeoMarkers, MS-289	1:100	1:50	-
CD117, PE	104D2	BD Biosciences, 332785	-	-	1:20
CD146	P1H12	Abcam, ab24577	1:1000	1:100	-
CD146, AF647	P1H12	BD Biosciences, 563619	-	-	1:20
CD326, PerCP/Cy5.5	9C4	BioLegend, 324214	-	-	1:20
CD326, BV421	EBA-1	BD Biosciences, 563180	-	-	1:20
ERα	1D5	Dako, M7047	1:100	-	-
Keratin 5	XM26	Novocastra, NCL-L-CK5	-	1:100	-
Keratin 5	-	Covance, PRB-160P	-	1:100	-
Keratin 7/8	CAM5.2	BD Biosciences, 345779	-	1:10-1:25	-
Keratin 14	LL002	Monosan,	1:100	1:25	

		MONX10687			
Keratin 15	LHK15	NeoMarkers, MS-1068	-	1:50	-
Keratin 17	E3	Dako, M7046	1:100	1:25	-
Keratin 19	A53-B/A2	BioLegend, 628502	-	1:25	-
Keratin 19	BA16	GenWay, GWBC266E	1:200	-	-
Keratin Ks20.8	Ks20.8	Dako, M7019	-	1:10	-
Ki-67	MIB-1	Dako, M7240	-	1:25	-
SSEA4	MC813-70	Millipore, MAB4304	-	1:25	-
Alexa Fluor 488 goat anti mouse IgG1	-	Invitrogen, A21121	-	1:500	-
Alexa Fluor 488 goat anti mouse IgG3	-	Invitrogen, A21151	-	1:500	-
Alexa Fluor 568 goat anti mouse IgG1	-	Invitrogen, A21124	-	1:500	-
Alexa Fluor 568 goat anti mouse IgG2a	-	Invitrogen, A21134	-	1:500	-

Alexa Fluor 568 goat anti mouse IgG2b	-	Invitrogen, A21144	-	1:500	-
Alexa Fluor 568 goat anti-rabbit IgG	-	Molecular Probes, A-11036	-	1:500	-
Alexa Fluor 647 goat anti-rabbit IgG2a	-	Invitrogen, A21241	-	1:500	-
Rhodamine Red goat anti-mouse IgG3	-	Jackson ImmunoResearch, 115-295-209	-	1:100	-